# Potential physical and chemical barriers to infection by the burrowing nematode *Radopholus similis* in roots of susceptible and resistant banana (*Musa* spp.)

N. Wuyts[a]*†, G. Lognay[b], M. Verscheure[c], M. Marlier[c], D. De Waele[a] and R. Swennen[a]

[a]*Laboratory of Tropical Crop Improvement, Division of Crop Biotechnics, Catholic University of Leuven (K.U. Leuven), Kasteelpark Arenberg 13, 3001 Leuven;* [b]*Unité de Chimie Analytique, Faculté Universitaire des Sciences Agronomiques de Gembloux, Passage des Déportés 2, 5030 Gembloux; and* [c]*Unité de Chimie Générale et Organique, Faculté Universitaire des Sciences Agronomiques de Gembloux, Passage des Déportés 2, 5030 Gembloux, Belgium*

Resistance in banana roots against the burrowing nematode *Radopholus similis* has been correlated in the past with the phenylpropanoid pathway of secondary metabolism, but quantitative chemical analyses to support histological data are lacking. Therefore, healthy and infected roots of two susceptible (Grande naine and Obino l'ewai) and three resistant cultivars (Yangambi km5, Pisang jari buaya and Calcutta 4) were extracted and chemically analysed for their lignin content and phenylpropanoid profile using a quantitative lignin assay, high performance liquid chromatography and liquid chromatography/mass spectrometry. Through histochemical staining phenylpropanoids were localized in root tissue. Compared to the susceptible cultivars, the resistant cultivars had constitutively significantly higher levels of lignin in the vascular bundle and cell-wall bound ferulic acid esters in the cortex. Infection-induced lignification was observed in the vascular bundles of all cultivars. The catecholamine dopamine was identified as a major metabolite in banana roots. Levels varied from 2·8 to 8·4 mg per g root fresh weight and were significantly higher in the resistant cultivars. Other compounds, tentatively identified as anthocyanidin-related, were present in high quantities and may, besides dopamine, make up the substrates for polyphenol oxidation products in necrotic tissue.

*Keywords*: dopamine, lignin, *Musa acuminata*, phenylpropanoids, *Radopholus similis*, resistance

## Introduction

The burrowing nematode *Radopholus similis* is one of the most important root pathogens of bananas (*Musa* spp.) causing severe yield losses in commercial and small-scale cultivation worldwide (Sarah *et al.*, 1996). Extensive application of chemical nematicides is the normal control practice in commercial plantations, but this has become highly questionable due to high costs, deteriorating soil health and general environmental issues. Resistant cultivars are considered a more sustainable management option, equally accessible for subsistence banana growers as for commercial producers. In the past fifteen years, some sources of resistance against *R. similis* have been identified within the genus *Musa*. Knowledge of resistance mechanism(s) in these plants could provide 'markers' to

*E-mail: nathalie.wuyts@scri.ac.uk

†Present address: Scottish Crop Research Institute, Invergowrie, Dundee, DD2 5DA, UK.

facilitate and speed up the screening of *Musa* germplasm and improved hybrids, and may lead to (metabolic) engineering for resistance in important cultivars.

Plant resistance to parasitic nematodes involves both physical and chemical barriers, which are either constitutively present or induced by infection (Giebel, 1982). As with other plant-pathogen interactions, a positive correlation has been established between host resistance and products of the phenylpropanoid pathway of plant secondary metabolism, frequently referred to as phenolic compounds. Host cell death and necrosis, accumulation of toxins, synthesis of phytoalexins and modification of cell walls are to a variable extent, depending on the plant species, ascribed to the phenylpropanoid metabolism (Trudgill, 1991; Nicholson & Hammerschmidt, 1992; Appel, 1993).

In previous research on resistance mechanisms in banana against the burrowing nematode *R. similis*, a greater number of cells containing phenolic compounds was counted in the resistant cultivars Yangambi km5 (*Musa acuminata* AAA) and Gros Michel (*Musa acuminata* AAA) than in susceptible cultivars (Mateille, 1994;

Table 1 Classification of *Musa* cultivars according to genome and group, host status towards *Radopholus* similis and root system characteristics

| Cultivar | Genome, group | ITC code[a] | Host status[b] | Root system (in hydroponics)[c] |
|---|---|---|---|---|
| Grande naine (GN) | AAA, Cavendish | 1256 | susceptible | intermediate between OEA and Ykm5, PJB and C4 |
| Obino l'ewai (OEA) | AAB, Plantain | 0109 | susceptible | fewer, longer laterals; high proportion nodal roots |
| Yangambi km5 (Ykm5) | AAA, Ibota | 1123 | resistant | fewer, longer laterals; high proportion secondary laterals |
| Pisang jari buaya (PJB) | AA, Pisang jari buaya | 0312 | resistant | many, short laterals; high proportion secondary laterals |
| Calcutta 4 (C4) | AA, burmannicoides | 0249 | resistant | many, short laterals; high proportion secondary laterals |

[a]Accession number at the International *Musa* Germplasm Collection, INIBAP Transit Centre (ITC), K.U. Leuven. Cultivars are described in Daniells *et al*. (2001). [b]Wehunt *et al*. (1978); Pinochet & Rowe (1979); Price (1994); Fogain & Gowen (1998); Stoffelen *et al*. (2000); Viaene *et al*. (2003). [c]Swennen *et al*. (1986); Stoffelen (2000).

Fogain & Gowen, 1996). In the resistant cultivar Pisang jari buaya (*Musa acuminata* AA) a greater number of cells with lignified walls was observed (Fogain & Gowen, 1996) and in Yangambi km5 resistance to penetration of the vascular bundle was attributed to the extensive presence of suberin in endodermal cell walls (Valette *et al*., 1997; 1998). Phenylphenalenone phytoalexins have been identified in *Musa acuminata* but adverse effects on nematode behaviour have not been reported (Binks *et al*., 1997). Finally, the host status of banana cultivars has been correlated with levels of hydroxycinnamic acids, flavonoids, dopamine and condensed tannins in roots (Valette *et al*., 1998; Collingborn *et al*., 2000). In the banana-*R. similis* interaction, a role for phenylpropanoids has been suggested, but generally based only on histochemical staining in root sections. Chemical analyses allowing proper identification and quantification of root compounds are lacking.

In this study, five banana cultivars of well-characterized host status for *R. similis* were included. Healthy and infected roots were extracted for a comparative, qualitative and quantitative analysis of their phenylpropanoid content, including lignin, hydroxycinnamic acids and flavonoids. Histochemical staining was applied for the localization of phenylpropanoids in root sections. Potential physical and chemical barriers were identified in banana roots and their significance for resistance against nematodes is discussed.

## Material and methods

### Plant growth and inoculation

Five *Musa* cultivars differing in genome, host status towards *R. similis* and root system characteristics were chosen (Table 1). Twenty plants per cultivar were included in the experiment. *In vitro* propagated plants were transplanted to pots filled with 2·5 L of a sterilized 2:1 potting soil-quartz sand mixture. To each pot, 1 g Osmocote®, a slow release fertilizer, was added. The pots were maintained in a greenhouse at a day/night temperature of 27/20°C and irrigated as needed. After 15 weeks of growth in the greenhouse, eight to ten plants of each cultivar were inoculated with nematodes. A highly aggressive strain of *R. similis* from banana plants in Uganda was used in the experiment (Fallas *et al*., 1995). The nematode was cultured in the laboratory on carrot discs (Speijer & De Waele, 1997). Nematodes were collected in distilled water from six-week-old carrot discs. The volume of the suspension was adjusted with distilled water to a concentration of 250 female nematodes per 500 $\mu$L. Plants were inoculated by pipetting 500 $\mu$L of the nematode suspension in each of four holes made in the growth medium around the plant base. Thus, 1000 female *R. similis* were inoculated per plant. Ten plants of each cultivar, not inoculated with nematodes, were maintained simultaneously with the infected plants in a randomized block design.

### Sample collection

Twelve weeks after inoculation with *R. similis*, root samples were collected. Root systems were carefully washed without rubbing to avoid loss of the root surface layer. Roots were weighed, chopped, snap-frozen in liquid nitrogen and stored at −80°C prior to chemical extraction. Part of the roots were kept for histochemical staining and the estimation of nematode numbers in roots. Nematodes were extracted from a 5 g subsample using the maceration-sieving technique (Coolen & D'Herde, 1972) and counted using a binocular microscope.

### Quantification of lignin

Frozen root samples were ground in pre-cooled (liquid nitrogen) jars of a ball mill (Mixer Mill MM 301, Retsch GmbH). Cell walls were isolated from a 500 mg subsample as described by Lange *et al*. (1995). The lignin content of root cell walls was assayed by derivatization of lignin with thioglycolic acid as described by Lange *et al*. (1995). Absorbance of samples was read at 280 nm against a blank in a NanoDrop spectrophotometer (ND-1000, NanoDrop Technologies). The lignin content (lignothioglycolic acid, LTGA) was expressed as $\mu$g lignin per mg cell wall dry weight (DW) using a calibration curve of alkali lignin (Sigma-Aldrich).

### Extraction of root samples

Soluble phenylpropanoids were extracted from 500 mg of ground root tissue in 1 mL 80% methanol (v/v) with

1·7% L-ascorbic acid (w/v). Preliminary studies had shown that the addition of an antioxidant was required to avoid oxidation of phenylpropanoids by endogenous polyphenol oxidase in root samples (N. Wuyts, unpublished data). Samples were shaken at 26°C for 2 h, followed by centrifugation at 16 000 *g* for 10 min. The supernatant was passed through 0·45 *μ*m PTE filters (Machery-Nagel) into HPLC-vials.

Phenylpropanoids bound by glycosylation or esterification were extracted using acid hydrolysis (Hertog *et al.*, 1992). Ground root samples of 500 mg were suspended in 800 *μ*L 62·5% methanol (v/v) and 200 *μ*L 6N HCl in a pyrex tube with a Teflon-coated cover. Air in the tube was replaced by helium. Together with the acid pH of the extraction buffer and high temperature, this prevented oxidation of phenylpropanoids. Tubes were incubated for 30 min at 90°C with regular shaking, followed by cooling on ice and the addition of 1 mL of absolute methanol. Samples were vortexed and passed through 0·45 *μ*m PTE filters into HPLC-vials.

### Chromatographic analysis of root extracts

HPLC analysis was carried out on an Agilent HP 1100 system (Hewlett Packard) using an Inertsil ODS2 (250 × 3 mm, particle size 5 *μ*m) reverse phase analytical column (Chrompack). Extracts (15 *μ*L) were separated at 25°C with a flow rate of 0·4 mL min$^{-1}$ using a gradient of acetonitrile in water (MilliQ water at pH 3·0 with phosphoric acid): 18% for 30 min, 45% for 12 min, 100% methanol for 1 min and back to 18% for 9 min. A diode array detector (Hewlett Packard) was used to record the online spectra (254, 280, 330, 366 and 450 nm) of compounds eluting from the column. Fluorescence detection of salicylic acid was carried out with an excitation wavelength of 305 nm and emission at 407 nm. Peak integration was carried out on HP ChemStations software using phenylpropanoid standards (Sigma-Aldrich). Peaks were tentatively identified by comparing their retention times and UV absorption spectra with those of standards. Samples were spiked with authentic compounds to support tentative identifications. Standard calibration curves were derived for quantification purposes. In the case of acid hydrolysed samples, standards were similarly hydrolysed to monitor degradation and avoid underestimation.

The proposed identifications were finally corroborated by HPLC/MS using an Esquire HCT ESI-Ion Trap mass spectrometer (Bruker Daltonics) coupled to an Agilent HP 1100 system and analysed with Bruker Daltonics Data Analysis 3·2 software. Analytical conditions were the same as above. However, formic acid (more volatile) was used instead of phosphoric acid. Column effluent was monitored in negative and positive ion modes. Major MS parameters were as follows: capillary voltage, 4500 V; amplitude, 1 V; drying gas, $N_2$; gas flow rate, 10 L min$^{-1}$; gas temperature, 365°C; nebulizer pressure, 50 psi; full-scan data acquisition, scanning from *m*/*z* 50 to 500.

### Histochemical staining of phenylpropanoids in root sections

Healthy and visibly infected roots were hand-cut at the root-corm junction, in the middle of the root, in the root elongation zone and at nematode lesions. Fresh-cut sections were either treated with 4% gluteraldehyde and viewed by bright-field microscopy or stained. Tissue localization of phenylpropanoids was done by treating sections with 0·25% (w/v) diphenylboric acid 2-aminoethyl ester (DPBA, Sigma-Aldrich) in MilliQ water with 0·02% (v/v) Triton X-100 (Peer *et al.*, 2001). The sections were visualized immediately with an epifluorescence microscope equipped with a DAPI filter (excitation 340–380 nm, suppression LP 430 nm, purple light) and a FITC filter (excitation 450–490 nm, suppression LP 520 nm, blue light). Fluorescence of different DPBA-conjugated phenylpropanoids was studied at the same position of the sections with both types of filters. The fluorescence colour of standard phenylpropanoids was determined by spotting 2 *μ*L of a 10 mM stock solution of the standards in absolute methanol with 2 *μ*L DPBA-staining solution on a TLC paper (WA Peer, Purdue University, West Lafayette, Indiana, USA, personal communication). The spots were visualized with an epifluorescence microscope using a DAPI and a FITC filter. The standards included caffeic acid, ferulic acid, sinapic acid, chlorogenic acid, phloretin (naringenin chalcone), naringenin, kaempferol, quercetin, myricetin, quercitrin (quercetin-3-rhamnoside), rutin (quercetin-3-rutinoside), catechin, epicatechin, pelargonidin chloride, tannic acid and dopamine (Sigma-Aldrich).

Lignin was localized in sections by applying both Mäule and Wiesner (phloroglucinol-HCl) staining according to standard protocols (Monties, 1989). Suberin was detected using a saturated alcohol solution of Sudan IV (Sigma-Aldrich). Stained root sections were examined by bright-field microscopy. Photo documentation of root sections was achieved with a SPOT RT CCD camera and SPOT RT software version 3·3 (Diagnostic Instruments).

### Statistical analysis

Data on the lignin content of roots were analysed using ANOVA. The Tukey test was applied for multiple comparisons of group means (Statistica® Release 6, Statsoft). For analysis of quantitative HPLC data, Kruskal-Wallis analysis of variance by ranks was applied. When the Kruskal-Wallis statistic was significant, multiple comparisons between treatments were calculated as described by Siegel & Castellan (1988).

## Results

### Root system description

The appearance of the root systems of the different cultivars confirmed earlier descriptions (Table 1). The root systems of cvs Grande naine (GN) and Obino l'ewai (OEA) were the smallest and least branched. Healthy

Table 2 Total weight and lignin content of healthy and *Radopholus similis*-infected roots of five *Musa* cultivars 27 weeks after planting

| Cultivar | Root system weight (g) | | | Lignin content ($\mu$g mg$^{-1}$ cell wall dry weight) | | |
|---|---|---|---|---|---|---|
| | −*R. similis* | +*R. similis* | | −*R. similis* | +*R. similis* | |
| Grande naine (GN) | 55 a | 69 a | ns | 71 a | 112 ab | ** |
| Obino l'ewai (OEA) | 85 ab | 79 ab | ns | 107 ab | 89 a | ns |
| Yangambi km5 (Ykm5) | 116 b | 98 ab | ns | 164 c | 129 bc | * |
| Pisang jari buaya (PJB) | 103 b | 85 ab | ns | 145 bc | 104 ab | ** |
| Calcutta 4 (C4) | 118 b | 104 b | ns | 137 bc | 157 c | ns |

Data are averages of eight to ten replicates. Data in the same column followed by the same letter are not significantly different according to the Tukey-test ($P \leq 0.001$ for −*R. similis*, $P \leq 0.05$ for +*R. similis*). *, **, ns indicate that the difference between treatments is significant at $P \leq 0.05$, 0.01 or not, respectively, according to the Tukey-test.

plants of GN had the lowest root weights, whereas cvs Yangambi km5 (Ykm5), Pisang jari buaya (PJB) and Calcutta 4 (C4) the highest (Table 2). In infected plants, only GN significantly differed in root weight from C4. Root system weight was not significantly different between healthy and infected plants of a cultivar.

For all cultivars, two types of roots were distinguished: young roots that had recently emerged from the corm, and older, mature roots that had already developed laterals. Although in general the young roots were short, compared to the older roots, they could reach a considerable length (approx. 15 cm) without developing laterals. Young roots were still white in colour and fragile, while older roots were creamy-brown and flexible, which suggested a different level of lignification. Young roots were not subjected to phenylpropanoid analysis as they represented an average of only 1% of the root system weight. The older roots of GN and OEA were less coloured and flexible than those of Ykm5, PJB and C4, again suggesting lower levels of lignification.

Nematode infection was confirmed by the numbers of nematodes extracted from roots (on average 1554 and 3041 nematodes and eggs per 100 g roots for cvs GN and OEA, respectively, and 285 and 42 nematodes and eggs per 100 g roots for cvs Ykm5 and C4, respectively). In PJB, there was very little visible damage to roots. Therefore, only those roots showing lesions were included for extraction of phenylpropanoids and nematode counts (5991 nematodes and eggs per 100 g roots).

### Lignin content of roots

As expected, the lignin content of the cell walls of young roots was less than that of older roots (4−6% and 7−16% of the cell wall dry weight in young and older roots, respectively). Healthy roots of cvs Ykm5, PJB and C4 had the highest lignin contents (Table 2). Roots of GN infected with *R. similis* had a 1·6-fold higher lignin content than healthy roots. Infected roots of Ykm5 and PJB, on the other hand, were significantly less lignified than healthy roots. For OEA and C4 the average lignin content of infected roots was lower and higher, respectively, than that of healthy roots but the differences were not significant ($P \leq 0.05$). Infected roots of C4 were the most

lignified, while the lignin content of infected PJB roots did not differ from infected GN or OEA roots. A significant correlation was found between root system weight and lignin content ($r = 0.43$; $P \leq 0.0001$).

### Localization of lignin in banana root sections

Lignified tissues were localized by means of histochemical staining of root cross sections and the type of lignin (syringyl or guaiacyl) prevailing in the tissues was tentatively identified on the basis of fluorescence colour and staining with lignin-specific dyes. In the roots of all cultivars, diverse stages of secondary wall formation and lignification were observed in the vascular bundles and endodermis. Secondary wall formation and lignification thereof started in xylem-associated parenchyma at the periphery of the vascular bundle in young roots (Fig. 1a) and progressed to the middle as xylem differentiation was completed (Fig. 1b). In mature roots, the endodermis showed U-shaped thickening of the inner tangential walls typical of monocotyledons (Fig. 1b,c). Cultivars could not be distinguished on the basis of histochemical staining of root sections, except that cell walls in the vascular bundle of Ykm5 roots were thicker than those of other cultivars.

Extended lignification of the vascular bundle and endodermis was observed in infected roots of all cultivars. Opposite lesions in the root cortex, endodermal cells showed U-shaped (tertiary) thickening even if the rest of the endodermal cells had not yet reached that stage (Fig. 1c). Cells in the pericycle of the vascular bundle, which were not thickened in healthy roots, became lignified opposite lesions in the cortex or in the whole vascular bundle in the case of heavy damage (Fig. 1c). In infected roots of C4, and only slightly less in those of Ykm5, cell walls in the vascular bundle were extremely thick compared to healthy roots and infected roots of the other cultivars (Fig. 1d). Thus, increased lignification seemed to be an effective barrier against nematode spread in the vascular bundle, as necrosis never reached beyond the outer cell layers (pericycle), even when the endodermis still showed no tertiary thickening.

Lignified cell walls fluoresce blue under UV-light. When stained with DPBA, however, syringyl lignin (related to
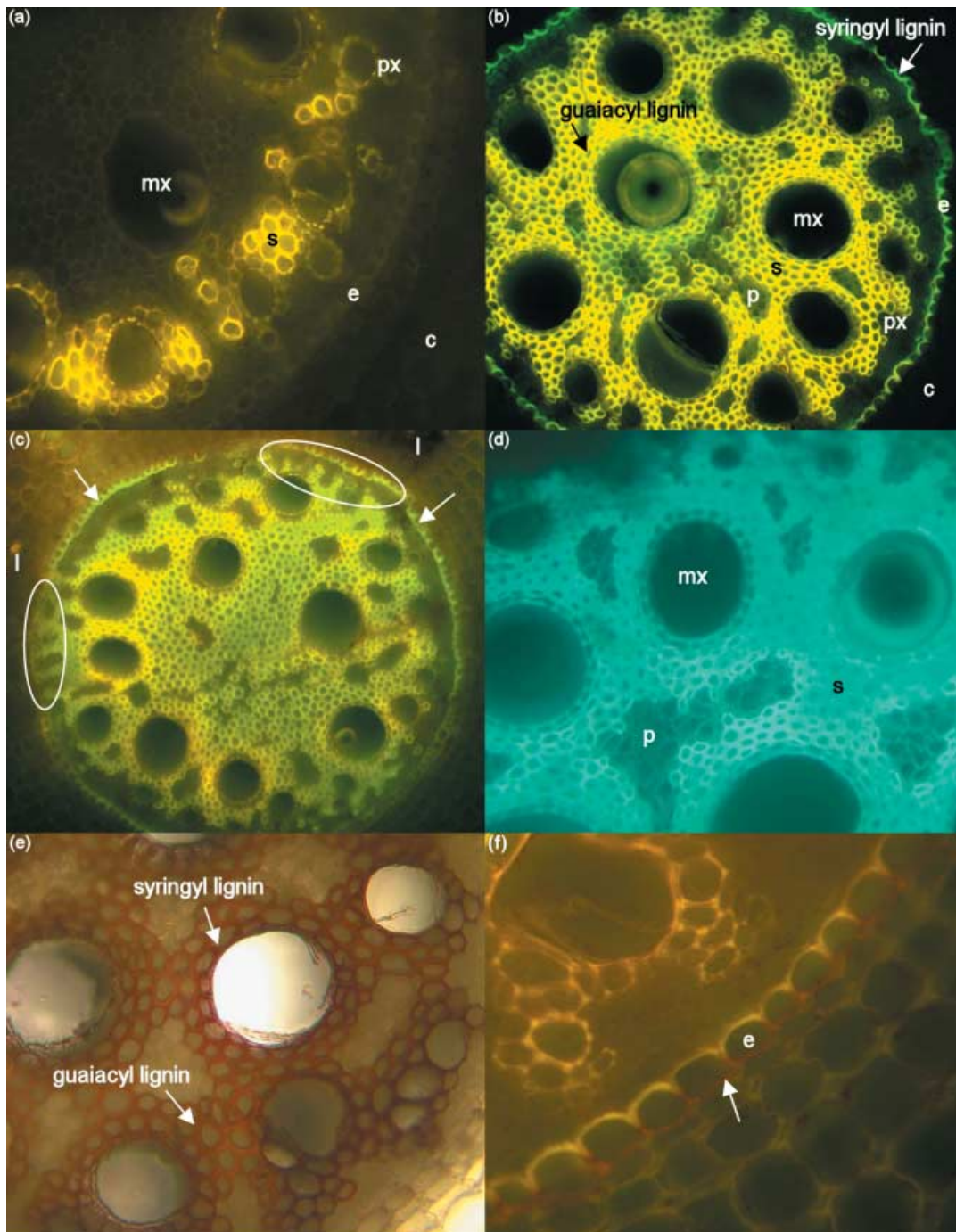
Figure 1 Tissue localization of lignin in cross sections of healthy and *Radopholus similis*-infected *Musa* roots. Fresh hand-cut sections were stained with DPBA and immediately visualized under an epifluorescence microscope with a FITC filter (a–c) or a DAPI filter (d), stained with the Mäule reagent and visualized with bright-field microscopy (e), or stained with Sudan IV and visualized under an epifluorescence microscope (f). (a) Xylem-associated cells in the vascular bundles of a young root starting to become lignified from the periphery towards the centre (healthy cv. Grande naine, ×100). (b) Healthy older root of Grande naine (×63) showing extensively lignified sclerenchyma and tertiary strengthening of the endodermis with lignin. (c) Infected root of cv. Yangambi km5 (×40) showing extended lignification of cells towards the pericycle (encircled) and formation of U-shaped thickenings in the endodermis (indicated by arrows) opposite lesions in the root cortex. In the sclerenchyma the ratio syringyl/ guaiacyl lignin is increased. (d) Detail of the vascular bundle of a cv. Calcutta 4 infected root (×100) showing the extremely thick secondary walls of sclerenchyma cells. (e) Localization of guaiacyl lignin in the sclerenchyma and syringyl lignin in the endodermis and xylem-bordering cells of a healthy cv. Pisang jari buaya root (×100). (f) Suberized walls of endodermal cells (cv. Yangambi km5, ×200) (indicated by an arrow). Suberin is masked on the inner tangential wall by the fluorescence of lignin. c-cortex, e-endodermis, l-lesion, mx-metaxylem, p-phloem, px-protoxylem, s-sclerenchyma.
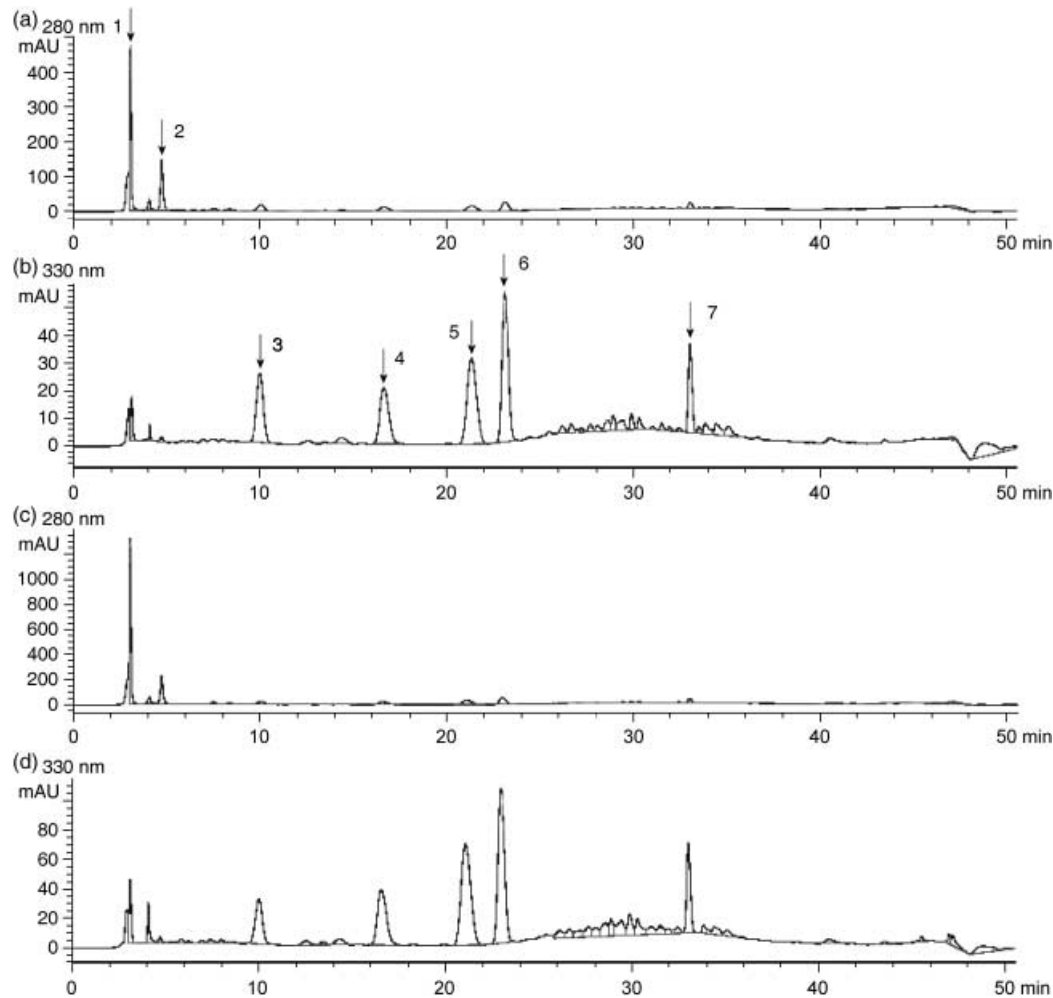
**Figure 2** HPLC-chromatograms of hydrolysed samples of *Radopholus similis*-infected roots of *Musa* cv. Grande naine (a and b) and cv. Calcutta 4 (c and d) 27 weeks after planting. Absorbance at 280 nm (a and c) and 330 nm (b and d). Peaks: 1, dopamine; 2, cyanidin-derived compound; 3, ferulic acid ester; 4, ferulic acid; 5, ferulic acid ester; 6, ferulic acid ester; 7, hydrolysis product of ferulic acid.

sinapic acid) and guaiacyl lignin (related to caffeic acid) fluoresce blue and greenish-white, respectively, when viewed through a DAPI filter and green and bright yellow, respectively, through a FITC filter (Fig. 1b). The distinction was confirmed by hydroxycinnamic acid standards and the Mäule reagent, which stains syringaldehyde residues in lignin bright red (Fig. 1e). In healthy fully matured roots, syringyl units were the major constituents of endodermal lignin, while guaiacyl lignin prevailed in sclerenchyma. Cells bordering xylem vessels were less lignified and contained syringyl lignin (Fig. 1e). In infected roots, the proportion of syringyl lignin increased in the endodermis and the vascular bundle (Fig. 1c).

Suberin was mainly detected in the exodermis and endodermis (Fig. 1f). Suberized walls also occurred in aerenchyma and isolated cells in the cortex. Suberization of sclerenchyma in the outer vascular bundle was observed in GN, PJB and C4. In infected roots, it was not possible

to distinguish the red colour of the Sudan dye from the red-brown colour of lesions.

### HPLC and LC/MS analyses

The HPLC method, as used for the banana root extracts, was highly reproducible: repeated injections of standard phenylpropanoid compounds with a 39 h delay were only slightly different in retention times (0–0·67%) and absorbance areas (0·1–1·1%). The repeatability of the whole procedure, including eight extractions of one and the same banana root sample and the analysis thereof, was also high: the coefficient of variation for the absorbance area of the major peaks in the chromatograms (Fig. 2) ranged from 3 to 10%. Through LC/MS analysis, the molecular weights of the major peaks of hydrolysed root extracts were established (Table 3) and some of them were unambiguously identified. For the others, fragmentation

**Table 3** ESI-MS data of phenylpropanoids in hydrolysed banana root samples

| Peak no.[a] | $t_R$ (min) | MS ions ($m/z$ positive mode (relative abundance, %)) | Compound |
|---|---|---|---|
| 1 | 3·0 | 154 (88), 137 (100) | dopamine |
| 2 | 4·7 | 287 (40), 144 (100) | cyanidin-related |
| 3 | 10·0 | 309 (100), 177 (15) | ferulic ester – [pentose]$_n$[b] |
| 4 | 16·6 | 195 (99), 177 (100) | ferulic acid |
| 5 | 21·3 | 309 (100), 177 (15) | ferulic ester – [pentose]$_n$ |
| 6 | 23·1 | 309 (100), 177 (12) | ferulic ester – [pentose]$_n$ |
| 7 | 33·0 | 209 (67), 177 (100) | ferulic acid – hydrolysis product |

[a]see Figure 2.

[b]n, unknown number.

patterns led to structure-hypotheses which need further confirmation. In the aforementioned analytical conditions, only a few 'diagnostic' ions were observed. For complete structural identification, the isolation of purified fractions of each molecule and careful complementary NMR spectrometric investigations are necessary. For that purpose, optimized LC separations should be applied.

The profile of soluble and bound phenylpropanoids of root samples, extracted by using 80% methanol or hydrolysis, respectively, only differed quantitatively, not qualitatively. The major soluble compound detected in banana root extracts was dopamine. The compound eluted at $t_R$ 3·0 min and showed a UV absorbance maximum at 280 nm. The retention time and UV absorption spectrum of the peak corresponded to the dopamine reference compound. LC/MS confirmed identification as dopamine (MW = 153 u), since the obtained MS ions corresponded to those of the reference compound (Table 3): a $[M + H]^+$ pseudomolecular ion at 154 u and a typical fragment at $m/z$ 137, corresponding to the loss of 16 u characteristic of an amino group (Wu *et al.*, 2003). In the profile of root samples extracted with 80% methanol, the dopamine peak co-eluted with ascorbic acid, which had been added to prevent oxidation by polyphenol oxidase (N. Wuyts, unpublished data). Observations on the dopamine peak area in hydrolysed root samples at 280 nm and by fluorescence detection ($\lambda_{Ex}$ 305 nm and $\lambda_{Em}$ 407 nm) allowed the calculation of the multiplication factor required to obtain the peak area at 280 nm in samples extracted with 80% methanol containing ascorbic acid, starting from the peak area resulting from fluorescence detection. The ratio between the two peak areas (280 nm/fluorescence) was 13·5 ± 1·1 for the root samples of the different cultivars. The dopamine content of banana root samples varied between 2·8 and 8·4 mg per g root fresh weight (Table 4). Ykm5, PJB and C4 had the highest dopamine levels in root samples, but the levels did not differ between healthy and infected roots (Table 4).

In the chromatograms of hydrolysed root samples, seven major peaks ($\lambda_{max}$ 280 nm and 330 nm) were detected (Fig. 2). Peak 1 ($t_R$ 3·0 min) was confirmed as dopamine

**Table 4** Content of peak 1 (dopamine), peak 2 ($t_R$ 4·7 min – $\lambda_{max}$ 280 nm) and peaks 3–7 (ferulic acid esters) of healthy and *Radopholus similis*-infected roots of five *Musa* cultivars 27 weeks after planting

| Peak 1 | Dopamine ($\mu$g g$^{-1}$ root fresh weight) | | |
|---|---|---|---|
| Cultivar | –*R. similis* | +*R. similis* | |
| Grande naine (GN) | 2821 a | 3772 a | ns |
| Obino l'ewai (OEA) | 3831 ab | 3666 a | ns |
| Yangambi km5 (Ykm5) | 6274 b | 6876 ab | ns |
| Pisang jari buaya (PJB) | 7477 b | 8362 b | ns |
| Calcutta 4 (C4) | 6367 b | 7805 b | ns |

| Peak 2 | $t_R$ 4·7 min – $\lambda_{max}$ 280 nm area (mAU.s)/g root fresh weight | | |
|---|---|---|---|
| Cultivar | –*R. similis* | +*R. similis* | |
| Grande naine (GN) | 5819 a | 3786 a | * |
| Obino l'ewai (OEA) | 4754 a | 4365 a | ns |
| Yangambi km5 (Ykm5) | 4717 a | 7162 a | * |
| Pisang jari buaya (PJB) | 5286 a | 5762 a | ns |
| Calcutta 4 (C4) | 7191 a | 5452 a | ns |

| Peak 3–7 | Ferulic acid esters area (mAU.s)/g root fresh weight | | |
|---|---|---|---|
| Cultivar | –*R. similis* | +*R. similis* | |
| Grande naine (GN) | 10012 a | 9417 a | ns |
| Obino l'ewai (OEA) | 9579 a | 10821 a | ns |
| Yangambi km5 (Ykm5) | 12618 b | 14115 b | ns |
| Pisang jari buaya (PJB) | 14663 b | 16042 b | ns |
| Calcutta 4 (C4) | 15234 b | 16618 b | ns |

Data are averages of three replicates. Data in the same column followed by the same letter are not significantly different according to Kruskal-Wallis ANOVA ($P \leq 0.05$). *, ns indicate that the difference between treatments is significant ($P \leq 0.05$) or not, respectively, according to Kruskal-Wallis ANOVA.

(see above). On the basis of retention time, UV absorption spectra and spiking with an authentic hydrolysed standard, peaks 4 ($t_R$ 16·6 min) and 7 ($t_R$ 33·0 min) were identified as ferulic acid and its hydrolysis degradation product, respectively. LC/MS analysis corroborated the nature of these molecules: the fragment at $m/z$ 195 corresponded to the $[M + H]^+$ pseudomolecular ion of ferulic acid while, according to Fang *et al.* (2002), the ion at $m/z$ 177 resulted from the loss of a hydroxyl moiety.

The retention times of peaks 3, 5 and 6 did not fit any of the available standard phenylpropanoid compounds. Their UV absorption spectra, however, indicated that they were related to caffeic acid, chlorogenic acid (caffeoyl-quinic acid) or ferulic acid. Their common fragment at $m/z$ 309 has previously been reported for ferulic acid esterified to a pentose moiety ($[M + H]^+$ = 309 u, MW = 308 u) (Bunzel *et al.*, 2002, 2005) and the characteristic $m/z$ 177 ion (see above) revealed ferulic acid as aglycone. Since no other typical ions have been observed within the scanned mass range, it was not possible to establish the number of sugar moieties. Absorbance areas for all ferulic acid-related peaks were summed and compared between cultivars and treatments (Table 4). Levels were not significantly different

between healthy and infected roots. For both, however, levels were significantly higher in Ykm5, PJB and C4.

Peak 2 ($t_R$ 4·7 min) showed an UV absorption spectrum typical of a catechol-like molecule with a strong $\lambda_{max}$ at 280 nm. LC/MS gave ions at *m/z* 144 and 287. The latter suggests the presence of the nonprotonated ion of cyanidin (Wu *et al*., 2004), while the former remains unattributed. Peak 2 represented 14–27% of the absorbance area in the HPLC chromatogram. No significant quantitative difference existed between the different cultivars. However, the levels in cv. GN were significantly lower in infected roots compared to healthy ones, while in Ykm5 levels were higher in infected roots (Table 4).

Finally, by LC/MS, ions indicative of anthocyanidin-related compounds were detected at $t_R$ 4·0 min, while an ion at *m/z* 126 detected at $t_R$ 2·3 min could correspond to the A-ring of the basic flavonoid structure reported as a common fragment of flavonoid-related compounds in LC/MS (Miketova *et al*., 2000).

### Localization of phenylpropanoids in banana root sections

Blue-fluorescing cell walls in DPBA-stained root sections (DAPI filter) indicated the presence of ferulic acid. They were detected in all cell types of the vascular bundle of young roots and in the elongation zone of older roots, where vascular differentiation is not yet completed. The walls of protophloem in particular contained high amounts of ferulic acid (Fig. 3a). In cvs PJB, Ykm5 and C4, all cortical cells contained ferulic acid in their walls, while, in GN and OEA, cell walls of the inner cortical layer, between the aerenchyma and the endodermis, frequently did not fluoresce. Hydroxycinnamic acids were also detected in walls of suberized cells in the exodermis. Sinapic acid (green fluorescence) was mainly found in the exodermis of root sections at the root-corm junction (Fig. 3b), while in all other parts caffeic acid (yellow fluorescence) prevailed (Fig. 3c).

Phenylpropanoid-containing cells were detected in young and older roots of all cultivars. Phenylpropanoids occurred in small granules or as an amorphous mass in cortical cells and in radial parenchymous cells around the lysogenous cavities of aerenchyma (Fig. 3d). Phenylpropanoid-containing cells were also found in the cortex of lateral roots inside nodal roots and in cells of nodal roots bordering laterals (Fig. 3e). Compounds showed yellow, orange and green fluorescence, which was previously ascribed to early intermediates of the flavonoid part of the phenylpropanoid pathway, such as naringenin, quercetin and kaempferol (flavonols) (Fig. 3d,e). These fluorescence colours were, however, shared with other flavonoids, among which were flavan-3-ols (catechin – green, epicatechin – yellow-green) and anthocyanidins (pelargonidin – bright orange). Based on the results obtained with LC/MS, it is likely that the fluorescing compounds in banana root sections are anthocyanidin-related rather than flavonol-related. The dopamine standard did not fluoresce when stained with DPBA and evaluated under an epifluorescence microscope with a FITC or DAPI filter. The oxidation product (quinone) of dopamine – when brought into contact with banana polyphenol oxidase – was, however, bright orange, as was the oxidation product of catechin.

Necrotic lesions in infected banana roots were surrounded by cells with yellow and orange fluorescing compounds in their intercellular spaces (Fig. 3f,g). This occurred in both susceptible and resistant cultivars but lesions with very little fluorescence were also found in the former. Lesions in infected roots of Ykm5 were surrounded by a layer of cells showing an accumulation of non-fluorescing dark brown and red material in cell walls and intercellular spaces, followed by cells with orange and yellow fluorescing compounds in intercellular spaces (Fig. 3g). Moreover, bright green and yellow fluorescence was detected in aerenchyma even at some distance from the necrotic area (Fig. 3h). In the lesioned cortex of infected PJB roots only, cells were detected which contained large granules filled with an unidentified compound showing green (DAPI filter) or faint yellow (FITC filter) fluorescence (Fig. 3i,j). PJB also differed from the other cultivars in the appearance of lesions. Lesioned areas were red-brown in roots of cvs GN, OEA, Ykm5 and C4, while in roots of PJB, lesions were surrounded by purple-blue cells and intercellular spaces.

## Discussion

Banana roots were (histo)chemically analyzed to gain insight into the role of phenylpropanoids in the resistance and susceptibility of selected banana cultivars to the burrowing nematode *R. similis*. Cross sections of nodal roots showed the structure of the vascular bundle and cortical parenchyma as described by Riopel & Steeves (1964) for roots of cv. Gros Michel (*Musa acuminata* AAA). No differences in the general organisation of root tissues were observed between susceptible and resistant cultivars (Mateille, 1994; Fogain & Gowen, 1996). The distinction between young and older roots in banana was reported by Fogain & Gowen (1996) and Lecompte *et al*. (2002). Roots with similar features have also been distinguished in field-grown maize and other monocotyledons (McCully, 1987).

Lignified cell walls are potential physical barriers to nematode migration and feeding as lignin would limit the access of nematode enzymes to cell wall polysaccharides (Ride, 1978). The resistant cultivars Ykm5, PJB and C4 were characterized by a highly branched root system, a significantly higher root weight and a significantly higher constitutive lignin content than the susceptible cvs GN and OEA. In older roots of both the resistant and susceptible cultivars, with fully differentiated xylem vessels, endodermal and sclerenchyma cells had thick, lignified secondary walls. Between older roots with an average lignin content of 13% and young roots with an average lignin content of 6%, varying levels of lignification were observed depending on the differentiation level of the vascular elements.
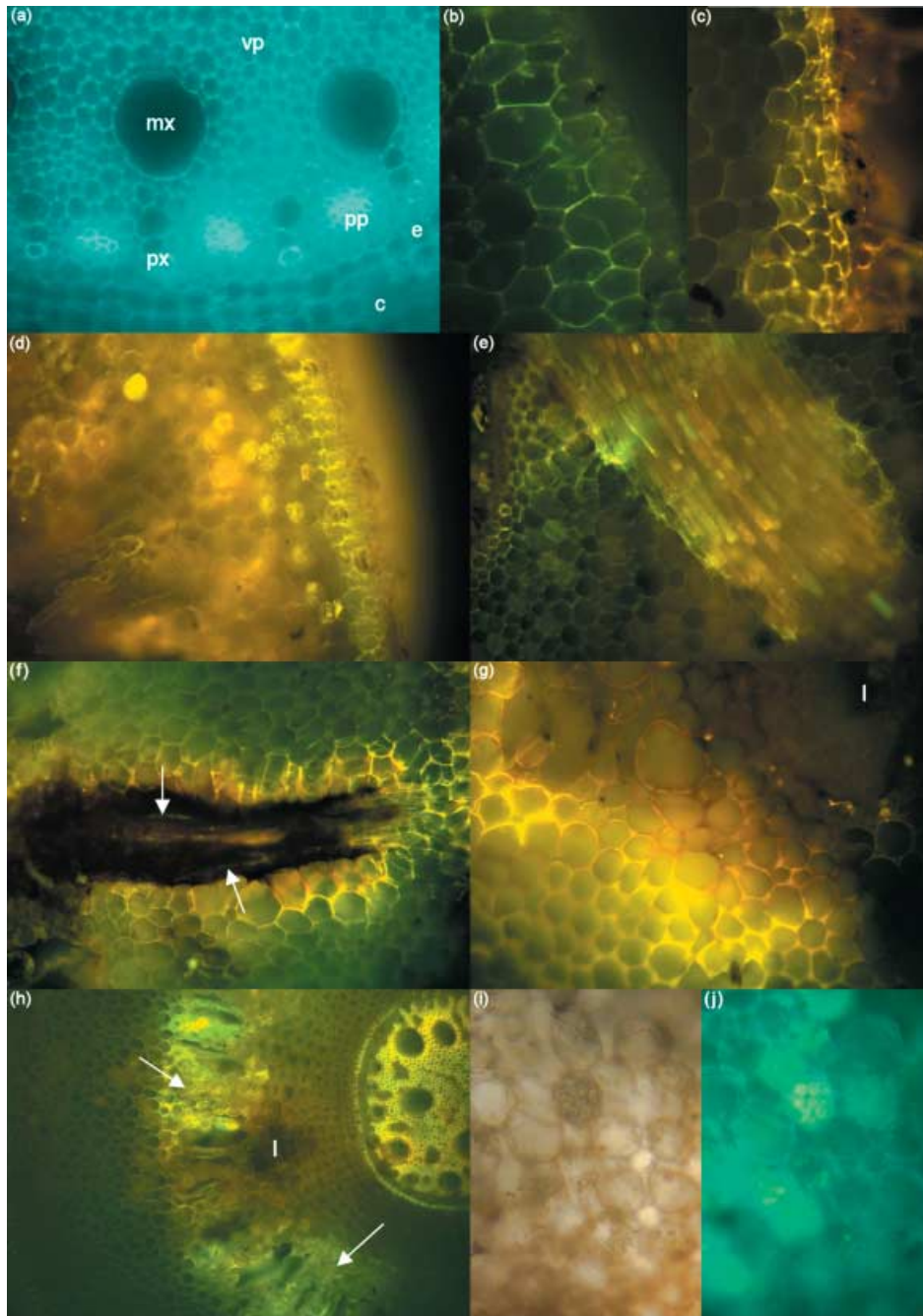
**Figure 3** Tissue localization of phenylpropanoids in cross sections of healthy and *Radopholus similis*-infected *Musa* roots. Fresh hand-cut sections were stained with DPBA and immediately visualized under an epifluorescence microscope with a DAPI filter (a, j) or a FITC filter (b–h), or visualized with bright-field microscopy (i). (a) Ferulic acid esterified to walls of vascular parenchyma and in particular protophloem in the developing vascular bundle of a healthy cv. Grande naine root (×100). (b) Sinapic acid bound to exodermis walls in a healthy cv. Pisang jari buaya root (×200). (c) Caffeic acid bound to exodermis walls in a healthy cv. Calcutta 4 root (×150). (d) Cortex and exodermis of a healthy young cv. Pisang jari buaya root showing phenylpropanoids in cells (yellow and orange fluorescence), either granular or amorphous (×100). (e) Phenylpropanoid-containing cells in the cortex of a lateral root inside a nodal root (healthy cv. Yangambi km5, ×63). (f) Necrotic area in the cortex of a lateral root inside a nodal root. Phenylpropanoids were detected in the intercellular spaces of cells bordering the lateral root. Nematodes were detected in the necrotic area of the lateral (indicated by arrows) (cv. Grande naine, ×63). (g) Detail of cells bordering a necrotic lesion with extensive amounts of phenylpropanoids in the intercellular spaces (cv. Yangambi km5, ×100). (h) Extensive phenylpropanoid accumulation (indicated by arrows) in the cortex of an infected cv. Yangambi km5 root, localized in aerenchyma next to the necrotic lesion (×40). (i) and (j) Cells containing large granules in a cv. Pisang jari buaya infected root (×300). These cells were found in the immediate vicinity of lesioned areas in the cortex of Pisang jari buaya roots only. c-cortex, e-endodermis, l-lesion, mx-metaxylem, pp-protophloem, px-protoxylem, vp-vascular parenchyma.

In sections of infected roots showing lesions in cortical cells, lignification of cells in the vascular bundle spread to the pericycle, and where the endodermis was not yet lignified, it became so opposite lesions. This was observed in both the resistant and susceptible cultivars and indicated a general defence mechanism to protect the vascular bundle from infection and/or damage. Moreover, in infected roots, the ratio of syringyl to guaiacyl lignin in cell walls of the vascular bundle was higher than in healthy roots, as has been noted in banana root-*Fusarium* interactions (de Ascensao & Dubery, 2000). The lignin content of infected roots, as determined by the thioglycolic acid assay, differed significantly from that of healthy roots for cvs GN, Ykm5 and PJB. In susceptible GN, the lignin content of infected roots increased to 158% of the levels in healthy roots and did not differ from levels in the resistant cvs Ykm5 and PJB, which were lower in infected roots (79 and 72% of the levels in healthy roots, respectively). This could indicate a redirection of the phenylpropanoid pathway from the synthesis of lignin precursors to other – possibly resistance-related – compounds.

A second possible physical (and chemical) barrier to nematode feeding and migration in the cortex of banana roots is provided by hydroxycinnamic acids covalently bound to cell wall polysaccharides. In monocotyledons, ferulic acid and *p*-coumaric acid esters substitute mainly arabinoxylans (hemicellulose). Upon acid or alkaline hydrolysis, feruloylated and *p*-coumaroylated arabinoxylan mono- and oligosaccharides are released (Ishii, 1997). The blue autofluorescence of ferulic acid was observed in banana root sections in the primary walls of cortical cells, cells of the immature vascular bundle in young roots, and in the elongation zone of older roots. In hydrolysed root samples of the resistant cultivars, significantly more ferulic acid and feruloylated pentose sugars (most likely arabinoses) were detected compared to the susceptible cultivars. The average content was slightly higher in infected roots, except for GN, but differences were not significant.

Covalently bound ferulic acids protect cell wall polysaccharides from enzymatic attack (Hartley & Jones, 1977). Plant parasitic nematodes secrete cell wall degrading enzymes, among which are cellulase, pectate lyase and polygalacturonase, during the infection process (Giebel, 1982). The presence of ferulic acids bound to cell walls may hinder the activity of these enzymes. Many bacteria and some fungi, such as *F. oxysporum*, produce feruloyl esterases to cleave the bonds that cross-link cell wall polysaccharides, so enhancing the access for cell wall degrading enzymes (Williamson *et al*., 1998). In banana roots, bacteria and fungi, including *F. oxysporum*, have been found in close association with *R. similis* during pathogenesis and are known to accelerate necrosis of root and corm tissue (Blake, 1966; Loridat, 1989; Sarah *et al*., 1996; Valette *et al*., 1997). If *R. similis*-associated bacteria or fungi aid in the degradation of cell walls by the production of feruloyl esterases, ferulic acid could be released from cell walls and accumulate to toxic levels. In *in vitro* bioassays, ferulic acid is a strong repellent at 350 $\mu$M, strongly inhibits motility and is toxic (LC$_{50}$ of 618 $\mu$M) to *R. similis*

(Wuyts *et al*., 2006a). Thus, ferulic acid could be a chemical barrier as well as a physical barrier to nematode infection.

Sample extraction and HPLC-analysis procedures were optimized to enable the detection and quantification of a broad range of simple phenylpropanoids and flavonoids, among which were hydroxycinnamic acids and flavonols, either present in a free form or bound to glycosides or cell walls. The major free compound detected in banana root samples was not a phenylpropanoid but dopamine, which is also called catecholamine because of its structural resemblance to the phenol catechol. The dopamine content of roots ranged from 2·8 to 8·4 mg per g root fresh weight, which is very high and comparable to levels in banana fruit from which dopamine was first extracted and identified (banana peel contains 3·8–13 mg dopamine per g fresh weight) (Kanazawa & Sakakibara, 2000). It has also been detected in roots by histochemical staining (*Musa* AAA, Gros Michel) (Mace, 1963; Valette *et al*., 1998) and in leaves and meristems (B. Panis, personal communication, Laboratory of Tropical Crop Improvement, Catholic University of Leuven, Belgium).

Dopamine is a potential chemical barrier to nematode infection. Roots of the resistant cultivars contained significantly higher levels of dopamine than the susceptible cultivars. In GN and OEA roots the levels were less than 50% of those in PJB roots. Average levels were slightly higher in infected roots of all cultivars, except OEA, but the differences were not significant. In *in vitro* bioassays, dopamine is not toxic to nematodes and does not inhibit motility or hatch. It acts as an attractant for *R. similis* at concentrations of ≤ 335 $\mu$M, but there are no data yet on the presence of dopamine in root exudates or its significance in the banana-*R. similis* interaction (Wuyts *et al*., 2006a). Furthermore, dopamine is a very good substrate for polyphenol oxidase isolated from banana roots, but (synthetic) melanin does not affect nematode behaviour either (Wuyts *et al*., 2006b; N. Wuyts, unpublished data). The intermediate quinones, formed by the action of polyphenol oxidase on dopamine, are more reactive and possibly toxic (Appel, 1993). In healthy tissues, dopamine is physically separated from polyphenol oxidase. Upon tissue damage, the cellular compartmentalization is lost and polyphenol oxidase from plastids can react with dopamine from the vacuole. In plant-nematode interactions, polyphenols are considered responsible for the brown and black pigmentation throughout cell walls and collapsed protoplasts in lesions and in adjoining live cells. They are thought to seal off infected tissue to limit secondary infection or spread of pathogens, inactivate nematode enzymes and to complex plant proteins which then become unavailable for nutrition (Bell, 1981; Townshend *et al*., 1989). The intensity of polyphenol formation was found to be correlated with resistance (Bell, 1981). In banana roots, especially in resistant cultivars, an ample supply of dopamine is available for the melanization of collapsed cells and walls of surrounding cells. In fluorescence microscopy observations, the walls of cells lining the lesions were dark, non-fluorescing or slightly orange, which supports this.

Large numbers of cells containing green, yellow and orange fluorescing granules or masses were observed in cortical cells of all cultivars. Dopamine does not auto-fluoresce or show fluorescence after treatment with DPBA-staining. Flavonols – kaempferol, quercetin, myricetin and their glycosides – which show these fluorescence colours, were only tentatively identified and in very small quantities in root samples. Other flavonoid standards showed very similar fluorescence too, among which were the anthocyanidin pelargonidin and the flavan-3-ols catechin and epicatechin. UV absorbance spectra and molecular weights obtained by LC/MS indicated the presence of these anthocyanidin-related compounds or their degradation products in large quantities. Whether these were anthocyanidins, flavan-3-ols, leucoanthocyanidins (flavan-3,4-diol precursors for the former two) or proanthocyanidins (condensed tannins) could not be determined by the extraction and HPLC analysis procedures that were used. The presence of anthocyanidins or their glycosides in roots can be expected from the red-brown and purple colour of lesions in infected roots. Further indications in support of the presence of proanthocyanidins were observed upon heating of root samples in acidic methanol: extracts turned bright red, which indicated the degradation of colourless proanthocyanidins into anthocyanidins (Porter et al., 1986). Collingborn et al. (2000) have reported the extraction and quantification of leucoanthocyanidins and proanthocyanidins from necrotic banana roots and correlate high levels of these compounds with the resistance found in cv. Kunnan (Musa acuminata AB). In preliminary experiments, using acid-methanol extraction for anthocyanidins (Adamse et al., 1989) and the butanol-HCl assay for the detection of proanthocyanidins (Collingborn et al., 2000), the presence of these compounds was confirmed in roots of GN, Ykm5 and PJB (Wuyts et al., 2005). Proanthocyanidins could be, besides melanin derived from dopamine, part of the polyphenol complex in necrotic tissue of banana roots. Proanthocyanidin formation from flavan-3-ols precursors is still unclear, but in one model epicatechin or catechin is converted to corresponding quinones by polyphenol oxidase. The quinones are then further metabolized to form proanthocyanidins (Dixon et al., 2005). Catechin is, besides dopamine, a very efficient substrate for banana root polyphenol oxidase (Wuyts et al., 2006b). Further support for proanthocyanidins as part of the polyphenol complex is found in banana fruit: polyphenols are primarily composed of catechin-residues co-polymerized with a small number of indole units (Andrews & Pridham, 1967).

In PJB roots lesions were purple-blue in colour compared to red-brown in the other cultivars, most likely due to a higher ratio of delphinidin versus cyanidin. Whether this has any significance for resistance needs to be assessed, as anthocyanidins are generally not associated with defence responses against pathogens, but rather with high visible light levels, cold stress and nutrient deficiency (Dixon & Paiva, 1995). In plant-fungal interactions, anthocyanidin accumulation has been observed in uninfected, healthy cells that surround lesions. Anthocyanidins, as antioxidants, are suggested to protect healthy plant tissue from toxic, oxidative metabolites that accumulate during the expression of defence or resistance (Hipskind et al., 1996). In nematode-infected roots of PJB, cells containing extremely large granules occurred in the cortex adjacent to lesions. These were not observed in any of the other cultivars. They indicated the accumulation of very large concentrations of (an) unidentified compound(s). Cells containing brown globules around necrotic tissue were found by Mateille (1994) in roots of the R. similis-resistant banana cv. Gros Michel (Musa acuminata AAA) and by Pinochet (1978) in plantain banana roots infected with Pratylenchus coffeae. The sequestration of large quantities of chemicals in cells close to infection sites is part of the defence strategy of plants as it primes these cells for cell wall modifications, cell death and the isolation of infection upon decompartmentalization and oxidation/activation (Wink, 1997; Beckman, 2000).

Two potential physical barriers to R. similis infection and migration were identified among phenylpropanoid compounds in banana roots: lignin and cell-wall bound ferulic acid esters. The resistant cvs Ykm5, PJB and C4 had constitutively higher levels of both of these compared to susceptible cvs GN and OEA. Lignification of the endodermis and cells within the vascular bundle was, however, induced in infected roots of all cultivars and seemed to be part of a general defence response to protect the vascular system. Further research on the lignin monomer content of banana roots is required, as well as on the ferulic acid esterified sugar moieties. Dopamine is a potential chemical barrier in banana roots, either directly or as a substrate for polymerization. Levels were high in roots and in particular in resistant cultivars. But, as mentioned above, more potential chemical barriers seem to be present in banana roots. Other extraction and HPLC analysis protocols adapted to flavan-3-ols, anthocyanidins and proanthocyanidins are required for further research into the biochemical basis for nematode resistance in banana. To date, no significant qualitative differences in the phenylpropanoid profile of resistant and susceptible banana cultivars have been observed. These do not necessarily need to exist as resistance could be determined by the rate and extent of reactions instead of their biochemical nature. Quantitative analysis of cell and tissue responses in the first hours and days after infection are required once a more complete picture of the biochemical potential of banana roots is obtained.

## Acknowledgements

## References

Adamse P, Peters JL, Jaspers PAPM, Van Tuinen A, Koornneef M, Kendrick RE, 1989. Photocontrol of anthocyanin synthesis in tomato seedlings: a genetic approach. *Photochemistry and Photobiology* **50**, 107–11.

Andrews RS, Pridham JB, 1967. Melanins from DOPA-containing plants. *Phytochemistry* **6**, 13–8.

Appel HM, 1993. Phenolics in ecological interactions: the importance of oxidation. *Journal of Chemical Ecology* **19**, 1521–52.

Beckman CH, 2000. Phenolic-storing cells: keys to programmed cell death and periderm formation in wilt disease resistance and in general defence responses in plants? *Physiological and Molecular Plant Pathology* **57**, 101–10.

Bell AA, 1981. Biochemical mechanisms of disease resistance. *Annual Review of Plant Physiology* **32**, 21–81.

Binks RH, Greenham JR, Luis JG, Simon SR, 1997. A phytoalexin from roots of *Musa acuminata* var. Pisang sipulu. *Phytochemistry* **45**, 47–9.

Blake CD, 1966. The histological changes in banana roots caused by *Radopholus similis* and *Helicotylenchus multicinctus*. *Nematologica* **12**, 129–37.

Bunzel M, Allerdings A, Sinwell V, Ralph J, Steinhart H, 2002. Cell wall hydroxycinnamates in wild rice (*Zizania aquatica* L.) insoluble dietary fibre. *European Food Research and Technology* **214**, 482–8.

Bunzel M, Ralph J, Steinhart H, 2005. Association of non-starch polysaccharides and ferulic acid in grain amaranth (*Amaranthus caudatus* L.) dietary fiber. *Molecular Nutrition and Food Research* **49**, 551–9.

Collingborn FMB, Gowen SR, Mueller-Harvey I, 2000. Investigations into the biochemical basis for nematode resistance in roots of three *Musa* cultivars in response to *Radopholus similis* infection. *Journal of Agricultural and Food Chemistry* **48**, 5297–301.

Coolen WA, D'Herde CJ, 1972. *A Method for Quantitative Extraction of Nematodes from Plant Tissue.* Gent, Belgium: State Agricultural Research Centre.

Daniells J, Jenny C, Karamura D, Tomekpe K, 2001. Musa*logue: a Catalogue of* Musa *Germplasm. Diversity in the Genus* Musa. Montpellier, France: The International Network for the Improvement of Banana and Plantain.

de Ascensao ARFDC, Dubery IA, 2000. Panama disease: cell wall reinforcement in banana roots in response to elicitors from *Fusarium oxysporum* f.sp. *cubense* race four. *Phytopathology* **90**, 1173–80.

Dixon RA, Paiva NL, 1995. Stress-induced phenylpropanoid metabolism. *The Plant Cell* **7**, 1085–97.

Dixon RA, Xie DY, Sharma SB, 2005. Proanthocyanidins – a final frontier in flavonoid research? *New Phytologist* **165**, 9–28.

Fallas GA, Sarah JL, Fargette M, 1995. Reproductive fitness and pathogenicity of eight *Radopholus similis* isolates on banana plants (*Musa* AAA cv. Poyo). *Nematropica* **25**, 135–41.

Fang N, Yu S, Prior RL, 2002. LC/MS/MS characterization of phenolic constituents in dried plums. *Journal of Agricultural and Food Chemistry* **50**, 3579–85.

Fogain R, Gowen SR, 1996. Investigations on possible mechanisms of resistance to nematodes in *Musa*. *Euphytica* **92**, 375–81.

Fogain R, Gowen SR, 1998. 'Yangambi km5' (*Musa* AAA, Ibota subgroup): a possible source of resistance to *Radopholus similis* and *Pratylenchus goodeyi*. *Fundamental and Applied Nematology* **21**, 75–80.

Giebel J, 1982. Mechanisms of resistance to plant nematodes. *Annual Review of Phytopathology* **20**, 257–79.

Hartley RD, Jones EC, 1977. Phenolic components and degradability of cell walls of grass and legume species. *Phytochemistry* **16**, 1531–4.

Hertog MGL, Hollman PCH, Venema DP, 1992. Optimization of a quantitative HPLC determination of potentially anticarcinogenic flavonoids in vegetables and fruits. *Journal of Agricultural and Food Chemistry* **40**, 1591–8.

Hipskind J, Wood K, Nicholson RL, 1996. Localized stimulation of anthocyanin accumulation and delineation of pathogen ingress in maize genetically resistant to *Bipolaris maydis* race O. *Physiological and Molecular Plant Pathology* **49**, 247–56.

Ishii T, 1997. Structure and functions of feruloylated polysaccharides. *Plant Science* **127**, 111–27.

Kanazawa K, Sakakibara H, 2000. High content of dopamine, a strong antioxidant, in Cavendish banana. *Journal of Agricultural and Food Chemistry* **48**, 844–8.

Lange BM, Lapierre C, Sandermann H, 1995. Elicitor-induced spruce stress lignin. *Plant Physiology* **108**, 1277–87.

Lecompte F, Vaucelle A, Pages L, Ozier-Lafontaine H, 2002. Number, position, diameter and initial direction of growth of primary roots in *Musa*. *Annals of Botany* **90**, 43–51.

Loridat P, 1989. Étude de la microflore fongique et des nématodes associés aux nécroses de l'appareil souterrain du bananier en Martinique. Mise en évidence du pouvoir pathogène du genre *Cylindrocladium*. *Fruits* **44**, 587–97.

Mace ME, 1963. Histochemical localization of phenols in healthy and diseased banana roots. *Physiologia Plantarum* **16**, 915–25.

Mateille T, 1994. Comparative host tissue reactions of *Musa acuminata* (AAA group) cvs Poyo and Gros Michel roots to three banana-parasitic nematodes. *Annals of Applied Biology* **124**, 65–73.

McCully MM, 1987. Selected aspects of the structure and development of field-grown roots with special reference to maize. In: Gregory PJ, Lake JV, Rose DA, eds. *Root Development and Function.* Cambridge, UK: Cambridge University Press, 53–70.

Miketova P, Schram KH, Whitney J *et al.*, 2000. Tandem mass spectrometry studies of green tea catechins. Identification of three minor components in the polyphenolic extract of green tea. *Journal of Mass Spectrometry* **35**, 860–9.

Monties B, 1989. Lignins. In: Dey PP, Harborne JB, eds. *Methods in Plant Biochemistry*, Vol. 1. London, UK: Academic Press, 113–57.

Nicholson RL, Hammerschmidt R, 1992. Phenolic compounds and their role in disease resistance. *Annual Review of Phytopathology* **30**, 369–89.

Peer WA, Brown DE, Tague BW *et al.*, 2001. Flavonoid accumulation patterns of *transparent testa* mutants of Arabidopsis. *Plant Physiology* **126**, 536–48.

Pinochet J, 1978. Histopathology of the root lesion nematode, *Pratylenchus coffeae*, on plantains, *Musa* AAB. *Nematologica* **24**, 331–40.

Pinochet J, Rowe PR, 1979. Progress in breeding for resistance to *Radopholus similis* on bananas. *Nematropica* **9**, 76–8.

Porter LJ, Hrstich LH, Chan BG, 1986. The conversion of procyanidins and prodelphinidins to cyanidin and delphinidin. *Phytochemistry* **25**, 223–30.

Price NS, 1994. Field trial evaluation of nematode susceptibility within *Musa*. *Fundamental and Applied Nematology* **17**, 391–6.

Ride JP, 1978. The role of cell wall alterations in resistance to fungi. *Annals of Applied Biology* **89**, 302–6.

Riopel JL, Steeves TA, 1964. Studies on the roots of *Musa acuminata* cv. Gros Michel: the anatomy and development of main roots. *Annals of Botany* **28**, 475–94.

Sarah JL, Pinochet J, Stanton J, 1996. The burrowing nematode of bananas, *Radopholus similis* Cobb, 1913. Musa *Pest Fact Sheet N° 1*. Montpellier, France: The International Network for the Improvement of Banana and Plantain.

Siegel S, Castellan NJ, 1988. *Nonparametric Statistics for the Behavioral Sciences*. New York, USA: McGraw-Hill Book Co.

Speijer PR, De Waele D, 1997. *Screening of* Musa *Germplasm for Resistance and Tolerance to Nematodes. INIBAP technical guidelines 1*. Montpellier, France: The International Network for the Improvement of Banana and Plantain.

Stoffelen R, 2000. *Early Screening of* Eumusa *and* Australimusa *Bananas Against Root-lesion and Root-knot Nematodes*. Leuven, Belgium: Catholic University of Leuven, PhD thesis.

Stoffelen R, Verlinden R, Pinochet J, Swennen RL, De Waele D, 2000. Host plant response of Fusarium wilt resistant *Musa* genotypes to *Radopholus similis* and *Pratylenchus coffeae*. *International Journal of Pest Management* **46**, 289–93.

Swennen R, De Langhe E, Janssen J, Decoene D, 1986. Study of the root development of some *Musa* cultivars in hydroponics. *Fruits* **41**, 515–24.

Townshend JL, Stobbs L, Carter R, 1989. Ultrastructural pathology of cells affected by *Pratylenchus penetrans* in alfalfa roots. *Journal of Nematology* **21**, 530–9.

Trudgill DL, 1991. Resistance to and tolerance of plant parasitic nematodes in plants. *Annual Review of Phytopathology* **29**, 167–92.

Valette C, Nicole M, Sarah JL, Boisseau M, Boher B, Fargette M, Geiger JP, 1997. Ultrastructure and cytochemistry of interactions between banana and the nematode *Radopholus similis*. *Fundamental and Applied Nematology* **21**, 65–77.

Valette C, Andary C, Geiger JP, Sarah JL, Nicole M, 1998. Histochemical and cytochemical investigations of phenols in roots of banana infected by the burrowing nematode *Radopholus similis*. *Phytopathology* **88**, 1141–8.

Viaene N, Durán LF, Rivera JM, Dueñas J, Rowe P, De Waele D, 2003. Responses of banana and plantain cultivars, lines and hybrids to the burrowing nematode *Radopholus similis*. *Nematology* **5**, 85–98.

Wehunt EJ, Hutchinson DJ, Edwards DI, 1978. Reaction of banana cultivars to the burrowing nematode (*Radopholus similis*). *Journal of Nematology* **10**, 368–70.

Williamson G, Faulds CB, Kroon PA, 1998. Specificity of ferulic acid (feruloyl) esterases. *Biochemical Society Transactions* **26**, 205–9.

Wink M, 1997. Compartmentation of secondary metabolites and xenobiotics in plant vacuoles. *Advances in Botanical Research* **25**, 141–69.

Wu HF, Chen CH, Lu LC, 2003. Probing the mechanisms of the self ion-molecule reactions of dopamine in an ion trap mass spectrometer. *Rapid Communications in Mass Spectrometry* **17**, 1479–82.

Wu X, Gu L, Prior RL, McKay S, 2004. Characterization of anthocyanins and proanthocyanidins in some cultivars of *Ribes*, *Aronia*, and *Sambucus* and their antioxidant capacity. *Journal of Agricultural and Food Chemistry* **52**, 7846–56.

Wuyts N, Lognay G, Sági L, De Waele D, Swennen R, 2005. Secondary metabolites in roots and implications for nematode resistance in banana (*Musa* spp.). In: Turner DW, Rosales FE, eds. *Banana Root System: Towards a Better Understanding for its Productive Management. Proceedings of an international symposium*. Montpellier, France: The International Network for the Improvement of Banana and Plantain, 238–46.

Wuyts N, Swennen R, De Waele D, 2006a. Effects of plant phenylpropanoid pathway products and selected terpenoids and alkaloids on the plant parasitic nematodes *Radopholus similis*, *Pratylenchus penetrans* and *Meloidogyne incognita*. *Nematology* **8**, 89–101.

Wuyts N, De Waele D, Swennen R, 2006b. Extraction and partial characterization of polyphenol oxidase from banana (*Musa acuminata* Grande naine) roots. *Plant Physiology and Biochemistry* **44**, 308–14.